Three-dimensional spatial imaging in multiphoton ionization rate measurements

Richard Bredy*, Howard A. Camp, and Hai Nguyen†

Department of Physics, J. R. Macdonald Laboratory, Kansas State University, Manhattan, Kansas 66506-2601

Takaaki Awata

Department of Physics, Naruto University of Education, Naruto, Tokushima 772-8502, Japan

Bing Shan, Zhenghu Chang, and B. D. DePaola

Department of Physics, J. R. Macdonald Laboratory, Kansas State University, Manhattan, Kansas 66506-2601

Received April 2, 2004; revised manuscript received May 28, 2004; accepted August 11, 2004

An experiment is described in which an apparatus is used to demonstrate the feasibility of measuring multiphoton photoionization rates in the interaction of short pulsed lasers with atoms or molecules. With this methodology, the ionization rate is measured as a function of the spatial position in the beam-waist region of the laser through the direct three-dimensional spatial imaging of the ionization events. Thus, if the spatial dependence of the laser beam intensity were known, a series of experiments could yield the intensity dependence of multiphoton ionization without the assumptions or errors that are generally inherent in the integration over one or more dimensions in the laser focal volume. © 2004 Optical Society of America

OCIS codes: 260.5210, 260.3230, 270.6620, 140.7090.

1. INTRODUCTION

The interaction of atoms or molecules with a femtosecond laser field has been investigated intensively in recent years, from both the experimental and the theoretical point of view.[1–6] For most of these experiments, the laser beam is focused to a waist inside an interaction region, and information about the interaction, such as the ionization rate, is deduced from experimental data that have been integrated over the entire focal volume. This could lead to large uncertainties in the measured intensity dependence of the interaction, since the laser focal volume includes a distribution of laser intensity. A way to reduce these uncertainties is to arrange a target volume that is smaller than the focal volume. Alternately, one must assume that the interaction is dominated by the highest intensity near the focal point. In some cases, this assumption is reasonable owing to the highly nonlinear effects of the process. However, it has been shown[7–9] that some ionization features, such as coherence effects, may be masked by integration over the entire focal volume. For reduction of the uncertainty in the intensity dependence of photoionization, several approaches have been employed.[10–13] Similar in idea, these approaches make use of small apertures, slits, two-dimensional position-sensitive detectors (PSDs), or time-of-flight (TOF) measurements to eliminate integration over one or two spatial dimensions.

In this paper, a new technique is described in which the true three-dimensional (3-D) spatial coordinate of each photoionized atom is measured. These data, when combined with a measurement of the laser intensity as a function of position, can be used to determine the ionization rate as a function of laser intensity. The technique consists of extracting the ionized atoms with an electrostatic lens and detecting them with a two-dimensional PSD. The PSD image determines two coordinates, whereas the TOF determines a third coordinate. The main difference between this new method and previously published ones is that the entire ionized region is imaged in all three dimensions, whereas previous techniques require integration over at least one dimension.

Details of the experimental setup are presented in Section 2. Measured characteristics of the apparatus are described in detail in Section 3, including the measured magnification of the electrostatic imaging lens and a measurement of the TOF to a position conversion factor. Finally, the effect of target temperature is discussed, and the validity of the method is demonstrated.

Except where otherwise indicated, the coordinate system of the laser beam is designated by (X_L, Y_L, Z_L), where Z_L represents the direction of propagation of the laser beam. The coordinate system (X, Y, Z) refers to the object space of the target, whereas the system (X_i, Y_i, t) refers to the image space. X_i, Y_i are the coordinates of a point on the PSD detector and are correlated with a detected ion having TOF t.

2. EXPERIMENTAL SETUP

A simplified schematic of the experimental setup is shown in Fig. 1. An exhaustive description of the apparatus can be found elsewhere.[14] Briefly, a 25-fs pulse[15] of 800-nm laser radiation at 1-kHz repetition rate is directed into an interaction chamber filled with Rb vapor. The ionized at-

oms are then extracted by an electrostatic lens and detected by a PSD. The Rb vapor is provided by a source canister that operates via a reduction reaction whose rate is controlled by a heater wire inside the canister.[16] The laser beam can be translated in X if the mirror and lens assembly are translated along the x axis. The focal point can be translated along the laser beam direction if only the lens is translated along Z_L. The base pressure of the chamber is 10^{-10} Torr, while the typical Rb vapor pressure is $\sim 10^{-9}$ Torr. Because the PSD used in these experiments is of the "single-hit" type,[17,18] the target thickness and the laser pulse energy are kept low enough that the count rate is typically less than 300 counts per second. This ensures that, on average, less than one target atom is ionized per laser pulse. This limitation can be reduced through the use of a "multihit" PSD.[19]

After spatial filtering and collimation, the laser beam of diameter 8 mm is focused by an $f = 200$ mm focal length lens before entering the chamber in a vertical plane and at an angle of 55° relative to the horizontal $(-Z)$ axis. Theoretically, for this geometry, the Rayleigh length Z_R was 0.64 mm and the beam waist $2W_0$ was 25.4 μm, giving a beam spot of 5.1×10^{-6} cm^2. The laser peak intensity I_p was 9.5×10^{11} W/cm^2. In fact, direct measurement of the 3-D beam profile with a CCD camera that was translated along Z_L revealed that the beam was slightly astigmatic. Using previous methodologies, in which one integrates over spatial coordinates, one would have had no recourse other than to assume that the laser beam was Gaussian. Here, however, one need not make such assumptions but can use the full spatial information gained in 3-D beam-profile measurements. The 200-mm-focal-length lens is mounted on a translation stage and can be moved along the laser beam direction Z_L. A translation of the mirror and lens together along the X_L axis translates the beam waist in the chamber but does not alter its position in Y_L or Z_L.

The ion optics system acts as a magnifying lens that extracts and then spatially images the ionized atoms. The system is composed of a solid plate (called the pusher plate) followed by a series of 34 metallic rings of thickness 1.0 mm, outer diameter 85 mm, and inner diameter 53 mm. Each of these electrodes is equally spaced, center to center, by 5.2 mm and connected in series by 1-MΩ resistors. The focal point of the laser is located at approximately at the center of the sixth electrode. A pusher voltage V_p is applied to the pusher plate, and an independent voltage called the focus voltage V_f is applied to the seventeenth electrode (called the focusing ring). The last electrode is grounded. The front of the PSD, located 1024 mm from the pusher plate, is also connected to ground. Consequently, this geometry defines three regions: a constant field extraction region (from the pusher plate to the focusing ring), a constant field focusing region (from the focusing ring to the last ring), and a field-free drift region (from the last ring to the front of the PSD). The interface between the first two regions is characterized by fringing fields that are resonsible for the spatial focusing of the ionized atoms. The ion optics system was modeled with the SIMION program.[20] For this work, $V_p = 300$ V and $V_f = 263$ V, which leads to $V_p/V_f = 1.14$. With this value, magnifications in the X and Y directions of roughly -3.6 were calculated at the PSD position. (The minus sign indicates that the PSD image is inverted with respect to the object.) As is shown in Section 3, the input angle of the laser beam inside the chamber presents an advantage: Breaking the symmetry of the system allows direct measurements of both the conversion between ion TOF and the object position in the Z direction, as well as a concurrent measurement of the magnification in Y.

The arrival of a laser pulse initiates data acquisition; it starts a time-digital converter and, following an appropriate delay, forces the reading of the PSD. A "hit" on the PSD generates the "stop" signal of the time-digital converter. The PSD is a resistive anode preceded by three 40-mm-diameter microchannel plates used in the Z-stack configuration. The PSD spatial resolution is 0.25 mm, and the TOF resolution is between 1 and 2 ns.

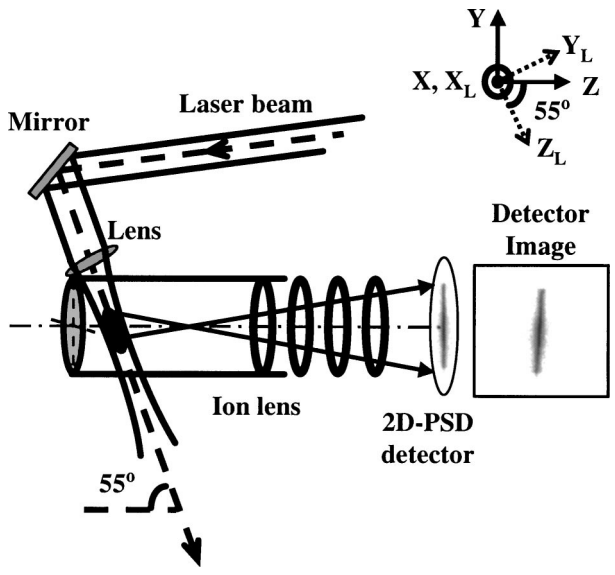

Fig. 1. Simplified schematic of the experimental setup.

3. SYSTEM CHARACTERISTICS

A. Electrostatic Lens

It is imperative to associate each PSD position X_i and Y_i, and TOF t, with a position in the 3-D object space (X, Y, Z). This requires a knowledge of the lens magnification M_X and M_Y along the X and Y axes as well as the TOF to Z conversion.

The magnification in X, M_X, of the electrostatic lens was measured through translation of the mirror and lens assembly by a known amount along the X axis and a direct measurement of the corresponding X_i shift of the image on the two-dimensional PSD. This method yields the absolute value of the X magnification:

$$|M_x| = 4.60 \pm 0.05. \tag{1}$$

In a similar measurement, the mirror position was kept fixed and the lens was translated along the laser beam axis in order to move the focal point along Z_L, yielding a measurement of the Y magnification:

$$|M_y| = 4.6 \pm 0.2. \tag{2}$$

If one knows the X and Y magnifications together with the PSD resolution, the resolution of the system in the object space can then be obtained: $\Delta x = \Delta y = 54\ \mu$m.

Translating the lens causes a shift of the image on the detector along the Y direction but also causes a shift of the TOF spectrum. Indeed, owing to the angle of the laser beam direction with respect to the horizontal plane, the ionized atoms have a shorter or longer TOF depending on the focal point position. Defining the zero of the Z axis to be the center of the sixth electrode of the ion lens, and taking into account the input angle of the laser beam, one can associate a Z coordinate of the focal point with a given position of the lens. This Z position can then be related to the centroid of the TOF spectrum measured for this particular lens position (Fig. 2). This gives the conversion from the TOF t to the Z position of the electrostatic lens:

$$Z = 6.36t - 353.14, \tag{3}$$

where Z is in millimeters, and t is in microseconds.

Taking into account the TOF resolution, the resolution Δz of the system in the object space for the Z direction is less than 13 μm.

From the previous results, it is clear that for each detected ion, its position on the PSD (X_i, Y_i) and its TOF t can be associated with a position in the 3-D object space (X, Y, Z). However, in order for one to obtain an accurate 3-D spatial image of the ionization region, the recoil momentum given to the ion during ionization must be negligible compared with that given by the extraction field. One can verify this condition experimentally by changing the polarization of the laser light; changing from linear to circular polarization should make no significant change to the measured image of the ionization region. This condition was experimentally verified. Clearly, the greater the extraction field, the more one may neglect the recoil momentum of the ion. However, in order to preserve good resolution in the TOF (and thus in the Z direction) the extraction field cannot be too large. The choice of V_p and V_f used in this work represents a compromise between these two constraints.

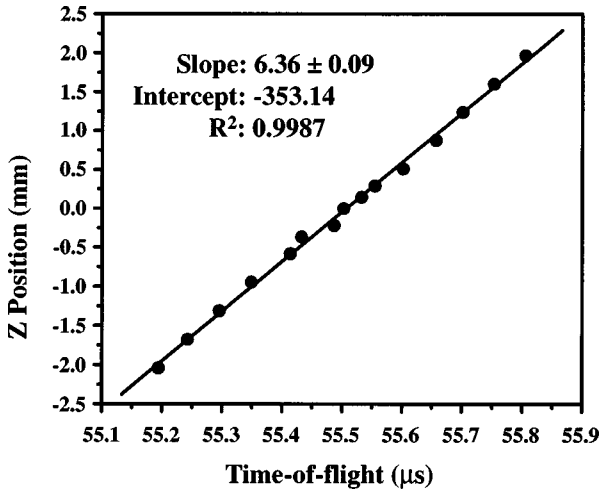

Fig. 2. Time-of-flight to Z conversion. The focal point is translated inside the chamber when the lens is translated along the direction of propagation of the laser beam. Owing to the input angle of the ion beam, the TOF spectrum of the ionized atoms is shifted depending on the focal-point position. This spectrum represents the Z position of the focal point as a function of the centroid of the TOF spectrum. TOF to Z conversion: $Z = 6.36t - 353.14$, with t in microseconds and Z in millimeters.

B. Effects of the Target Temperature

Thus far, only the physical limits of detector and timing resolution have been considered in order to estimate the best-case spatial resolution. In this section, limitation to resolution associated with nonzero target temperature will be considered.

Figure 3(a) represents a typical image of the ionization region. Figure 3(b) [3(c)] is a projection of the detector image onto the Y_i axis (X_i axis) and represents the yield of ionized atoms along the Y_i axis (X_i axis). Figure 3(d) represents the TOF spectrum associated with the detector image. As shown in Figs. 3(b) and 3(c), a software gate of size 0.636 mm was set on the X_i and Y_i axes, which corresponds to a 0.138-mm gate on the X and Y axes in object space. The TOF spectrum associated with the ions detected inside the X and Y gates is also shown in Fig. 3(d). Surprisingly, the width remains broad compared with the TOF of the total spectrum. If the size of the laser beam waist is taken into account, and if the ionization is assumed to occur mostly inside this beam area, the width of the TOF for the gated ions is expected to be ~19 ns. The actual width of 600 ns is due to the thermal energy of the target atoms, which is ~0.1 eV for these experimental conditions. Indeed, the Rb atoms are formed at ~780 K owing to the heater wire inside the canister source.

From Fig. 3 it is clear that the spatial (X, Y) and time (Z) resolutions are not nearly as good as those estimated in Section 2. The assumption that the poor resolution is due to finite target temperature was verified by repetition of the measurements of Fig. 3 on a laser-cooled target (MOT). The choice of the cooling method was influenced by the fact that the experimental setup described above is actually a part of a more complicated system that combines a MOT, an ion beam line, and a momentum spectrometer for the purpose of studying ion–atom collisions.[21–24] Since the purpose of the present work differs from such research, experimental details will not be described here but can be found elsewhere.[14,25]

The Rb target atoms are cooled down inside the MOT to a temperature of ~200 μK. The size of the cloud of cold atoms is ~0.5 mm in diameter. Results are shown in Fig. 4. Figure 4(a) represents the image of the ionization region. The intense spot near the bottom of the image is due to the cloud of cold atoms, which was not located exactly at the focal point of the laser beam. The image of the entire ionization region is slightly wider than that seen in Fig. 3(a) because of the distortion of the ion trajectories introduced by the B-field gradient applied to trap the atoms. As in Fig. 3, Fig. 4(b) [4(c)] represents the projection of the detector image onto the Y_i axis (X_i axis), and Fig. 4(d) represents the TOF spectrum. The Rb vapor is composed of two isotopes, ^{85}Rb and ^{87}Rb, but only the ^{87}Rb atoms are cooled and trapped inside the MOT. On the TOF spectrum, the broad peak extending from 2500 ns to 4500 ns corresponds mainly to the ionized background ^{85}Rb atoms that are still "hot," whereas the narrow peak corresponds to the cold ionized ^{87}Rb.

Software gates of identical size to the previous ones are set on the X_i and Y_i axes, and the TOF spectrum of the detected atoms inside both gates is shown in Fig. 4(d). The width of the gated TOF (21 ns) is now in very good agreement with the expected width relative to the gate size (19 ns).

From these results, it is clear that cold target atoms are necessary for complete realization of the spatial resolving potential of the system. Using a MOT is probably not the most efficient way to measure the ionization rate as a function of the laser intensity, since the target may not overlap with the entire laser beam. In principle, one can use a very localized MOT target (in order to neglect density variations in the target) that can be moved along the path of the laser beam to probe all of the laser beam area. However, this method supposes a very good control of the MOT position, and the normalization of the results can lead to important uncertainties. It seems that the simplest and yet most useful system would employ a precooled supersonic expansion jet, as is commonly used in COLTRIMS experiments.[26,27] A further improvement would be to build an ion lens system that has an even larger magnification in order to improve the resolution in the object space. To obtain the ionization rate as a function of the intensity of the laser field, one would then associate, for each TOF and position on the PSD, the number of detected ions $R(X_i, Y_i, t)$ to a position (X, Y, Z) on the object space. A map of the intensity laser field $I(X, Y, Z)$ can be obtained independently. The ionization rate $R(X, Y, Z)$ can then be compared with the laser intensity map $I(X, Y, Z)$ to get the ionization rate as a function of laser intensity $R(I)$.

4. CONCLUSION

The ionization rate of atoms or molecules as a function of the intensity inside the field of a femtosecond laser can be obtained with an ion imaging technique. A true 3-D spatial image of the ionized region is obtained with an electrostatic lens in combination with a TOF technique and a PSD. In this paper, the experimental setup and the method used to characterize the parameters of the electrostatic lens have been described. A larger detector and/or modified ion optics could be used to further increase the system's magnification. In addition, a study of the system shows the importance of having a cold target in order to reach the spatial resolution required to give an accurate measurement of the ionization rate as a function of the laser intensity. For cold atoms or molecules, a spatial resolution of 0.68 mm in X and Y and 0.13 mm in Z

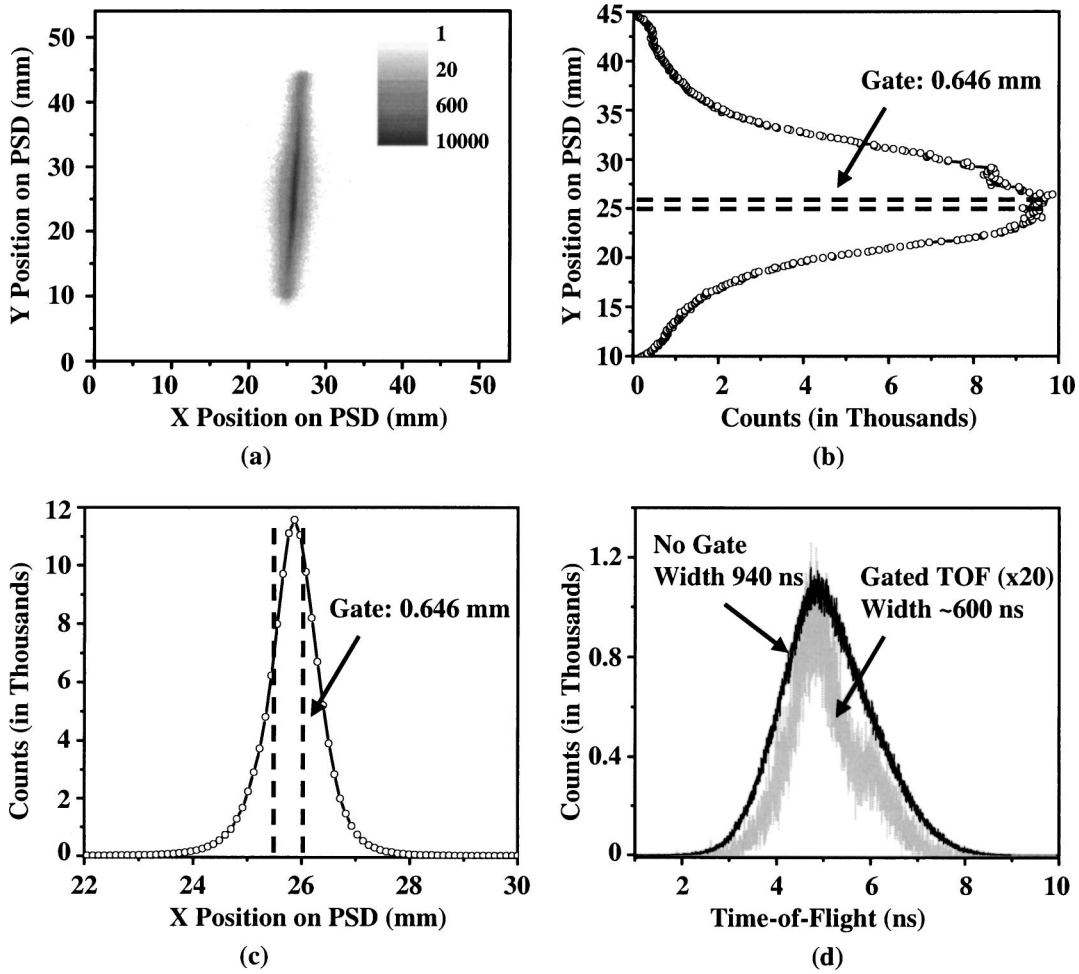

Fig. 3. Use of a 700 K Rb vapor as a target. (a), typical PSD image of the ionized region; (b), projection on the Y_i axis; (c), projection on the X_i axis; (d), corresponding TOF spectra. The curve labeled "gated TOF" corresponds to the TOF of the ions detected inside a $\Delta X_i = 0.636$ mm by $\Delta Y_i = 0.636$ mm gate set on the detector image. Gate positions are shown on each projection.

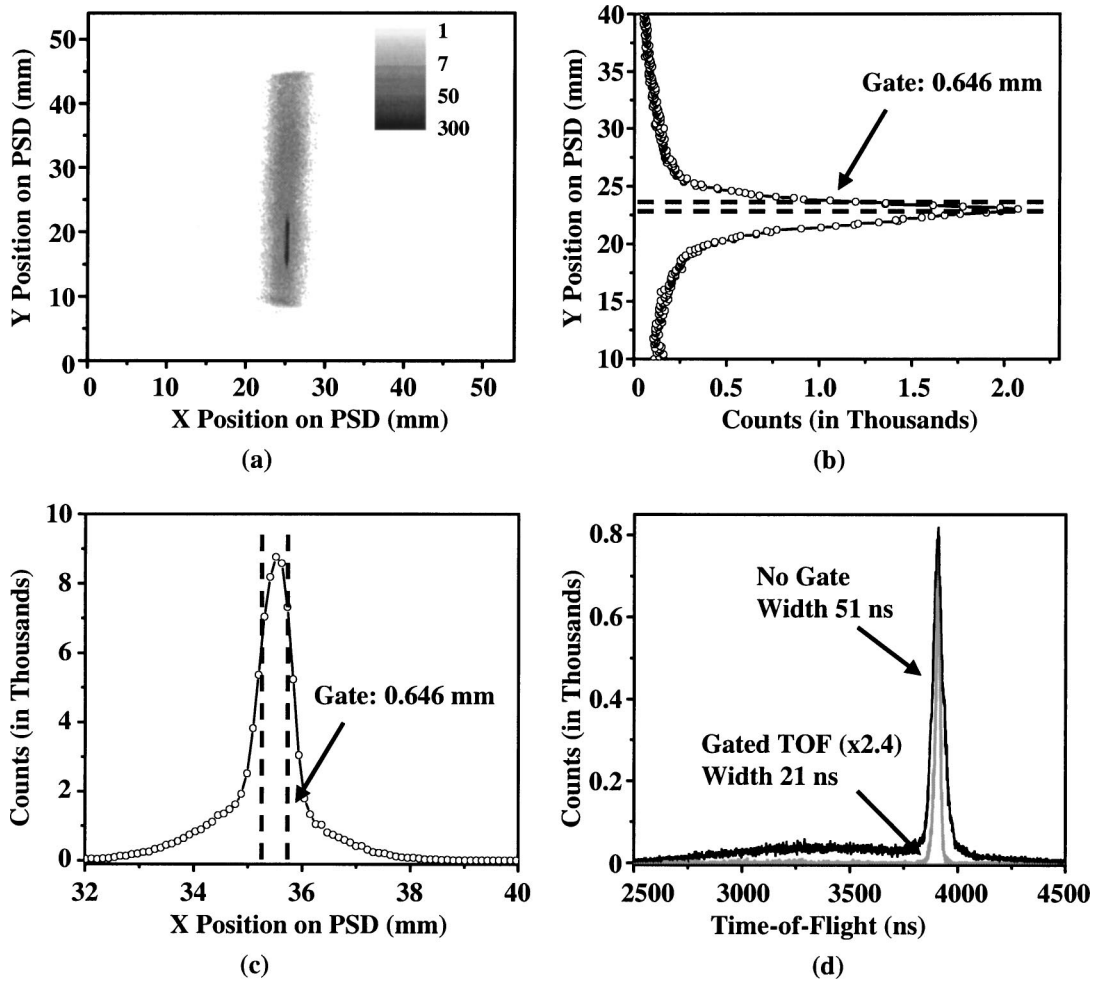

Fig. 4. As in Fig. 3, but with 200 μK ^{87}Rb atoms in a MOT. The measured TOF width is now consistent with estimates.

are obtained. In principle, any atomic or molecular vapor target can be studied with this kind of system, which is relatively easy to construct. Varying the target gas pressure would allow one to measure ionization rates for different intensity ranges. Once the ionization rate versus intensity is known, this methodology could then be turned around and used to map out the 3-D intensity profile of the laser. This same apparatus can also be used for momentum imaging in photoionization experiments.[5] Moreover, the method can be extended to the study of double and triple ionization, since the TOF technique allows the separation of these different processes.

ACKNOWLEDGMENTS

This work was supported by the Chemical Sciences, Geosciences, and Biosciences Division, Office of Basic Energy Sciences, Office of Science, U.S. Department of Energy. The laser facility was partially supported by a National Science Foundation Major Research Instrumentation grant. T. Awata is supported by the Ministry of Education, Culture, Sports, Science, and Technology of Japan.

B. D. DePaola's e-mail address is depaola @phys.ksu.edu.

*Present address: Laboratoire de Spectrométrie Ionique et Moléculaire, Unité Mixte de Recherche (UMR 5579), Centre National de la Recherche Scientifique, Université Claude Bernard Lyon 1, 69622 Villeurbanne, France.

†Present address, Laboratoire Charles–Fabry, Unité Mixte de Recherche (UMR 8501), Centre National de la Recherche Scientifique, Institut d'Optique, Universite de Paris-Sud, 91403 Orsay, Cedex, France.

REFERENCES AND NOTES

1. C. Guo, M. Li, J. P. Nibarger, and G. N. Gibson, "Single and double ionization of diatomic molecules in strong laser fields," Phys. Rev. A **58**, R4271–R4274 (1998).
2. X. M. Tong, Z. X. Zhao, and C. D. Lin, "Theory of molecular tunneling ionization," Phys. Rev. A **66**, 033402 (2002).
3. I. V. Litvinyuk, K. F. Lee, P. W. Dooley, D. M. Rayner, D. M. Villeneuve, and P. B. Corkum, "Alignment-dependent strong field ionization of molecules," Phys. Rev. Lett. **90**, 233003 (2003).
4. X. M. Tong and S. I. Chu, "Probing the spectral and temporal structures of high-order harmonic generation in intense laser pulses," Phys. Rev. A **61**, 021802 (2000).
5. C. Ellert and P. B. Corkum, "Disentangling molecular alignment and enhanced ionization in intense laser fields," Phys. Rev. A **59**, R3170–R3173 (1999).

6. E. Wells, M. J. DeWitt, and R. R. Jones, "Comparison of intense-field ionization of diatomic molecules and rare-gas atoms," Phys. Rev. A **66**, 013409 (2002).
7. R. R. Jones, "Multiphoton ionization enchancement using two phase-coherent laser pulses," Phys. Rev. Lett. **75**, 1491–1494 (1995).
8. A. Talebpour, C.-Y. Chien, and S. L. Chin, "Population trapping in rare gases," J. Phys. B **29**, 5725–5733 (1996).
9. P. Hansch and L. D. Woerkom, "High-precision intensity-selective observation of multiphoton ionization: a new method of photoelectron spectroscopy," Opt. Lett. **21**, 1286–1288 (1996).
10. P. Hansch, M. A. Walker, and L. D. Woerkom, "Spatially dependent multiphoton multiple ionization," Phys. Rev. A **54**, R2559 (1996).
11. C. J. Uiterwaal, Behlen Laboratory B56, University of Nebraska-Lincoln, Lincoln, Nebr. 68588 (personal communication, 2003).
12. M. A. Walker, P. Hansch, and L. D. Woerkom, "Intensity-resolved multiphoton ionization: circumventing spatial averaging," Phys. Rev. A **57**, R701–R704 (1998).
13. S. M. Hankin, D. M. Villeneuve, P. B. Corkum, and D. M. Rayner, "Intense-field laser ionization rates in atoms and molecules," Phys. Rev. A **64**, 013405 (2001).
14. H. Nguyen, X. Fléchard, R. Brédy, H. A. Camp, and B. D. DePaola, "Target recoil ion momentum spectroscopy using magneto-optically trapped atoms," Rev. Sci. Instrum. **70**, 032704 (2004).
15. The pulse width reported here is only approximate. For the purposes of this work, the exact pulse width is not relevant.
16. SAES Getters USA Inc., 1222 East Cheyenne Mountain Blvd., Colorado Springs, Colo. 80906.
17. H. C. Straub, M. A. Mangan, B. G. Lindsay, K. A. Smith, and R. F. Stebbings, "Absolute detection efficiency of a microchannel plate detector for kilo-electron volt energy ions," Rev. Sci. Instrum. **70**, 4238–4240 (1999).
18. Del Mar Ventures, 12595 Ruette Alliante 148, San Diego, Calif. 92130.
19. O. Jagutzki, V. Mergel, K. Ullmann-Pfelger, L. Spielberger, U. Meyer, R. Dörner, and H. Schmidt-Böcking, "Fast position and time-resolved read-out of microchannelplates with the delay-line techniques for single-particle and photon detection," in *Imaging Spectrometry IV*, M. R. Descour and S. S. Shen, eds., Proc. SPIE **3438**, 322–333 (1998).
20. The SIMION 3D Version 6.113 software package was developed by D. A. Dahl, MS 2208.
21. X. Fléchard, H. Nguyen, E. Wells, I. Ben-Itzhak, and B. D. DePaola, "Kinematically complete charge exchange experiment in the Cs^+ + Rb collision system using a MOT target," Phys. Rev. Lett. **87**, 123203 (2001).
22. X. Fléchard, H. Nguyen, R. Brédy, S. R. Lundeen, M. Stauffer, H. A. Camp, C. W. Fehrenbach, and B. D. DePaola, "State selective charge transfer cross sections for Na^+ with excited rubidium: A unique diagnostic of the population dynamics of a magneto-optical trap," Phys. Rev. Lett. **91**, 243005 (2003).
23. M. van der Poel, C. V. Nielsen, M.-A. Gearba, and N. Andersen, "Fraunhofer diffraction of atomic matter waves: electron transfer studies with a laser cooled target," Phys. Rev. Lett. **87**, 123201 (2001).
24. J. W. Turkstra, R. Hoekstra, D. Meyer, R. Morgenstern, and R. E. Olson, "Recoil momentum spectroscopy of highly charged ion collisions on magneto-optically trapped Na," Phys. Rev. Lett. **87**, 123202 (2001).
25. H. Nguyen, "Magneto optical trap recoil ion momentum spectroscopy," Ph.D. dissertation (Kansas State University, Manhattan, Kansas, 2003).
26. V. Mergel, Diploma Thesis, Johann-Wolfgang-Goethe Universität Frankfurt (unpublished 1994).
27. V. Mergel, R. Dörner, J. Ullrich, O. Jagutzki, S. Lencinas, S. Nüttgens, L. Spielberger, M. Unverzagt, C. L. Cocke, R. E. Olson, M. Schulz, U. Buck, E. Zanger, W. Theisinger, M. Isser, S. Geis, and H. Schmidt-Böcking, "State selective scattering angle dependent capture cross sections measured by cold target recoil ion momentum spectroscopy," Phys. Rev. Lett. **74**, 2200–2203 (1995).